



Get Clarity On Generics

Cost-Effective CT & MRI Contrast Agents

 **FRESENIUS
KABI**

[WATCH VIDEO](#)

AJNR

Spinal Cord Compression by Tophaceous Gout with Fluorodeoxyglucose–Positron-Emission Tomographic/MR Fusion Imaging

T. Popovich, J.S. Carpenter, A.T. Rai, L.V. Carson, H.J. Williams and G.D. Marano

This information is current as of August 7, 2025.

AJNR Am J Neuroradiol 2006, 27 (6) 1201-1203
<http://www.ajnr.org/content/27/6/1201>

CASE REPORT

T. Popovich
J.S. Carpenter
A.T. Rai
L.V. Carson
H.J. Williams
G.D. Marano

Spinal Cord Compression by Tophaceous Gout with Fluorodeoxyglucose–Positron-Emission Tomographic/MR Fusion Imaging

SUMMARY: A 36-year-old woman presented with lower extremity paralysis. Her past medical history included gout. Conventional radiography and MR imaging revealed bone erosion and soft tissue lesions of the thoracic spine. Fluorodeoxyglucose–positron-emission tomographic (FDG-PET) images revealed hypermetabolic lesions of the thoracic spine. A CT-guided biopsy was diagnostic for inflammatory tophaceous gout. This case describes the CT, MR, and FDG-PET imaging characteristics of acute inflammatory gout. FDG-PET imaging characteristics of this disorder have not been previously described.

Gouty spinal stenosis is a rare cause of spinal cord compression, with less than 25 cases reported in the literature. We report a case of thoracic spinal cord compression in a 36-year-old woman with a history of uncontrolled gout, with inclusion of CT, MR, and positron-emission tomography (PET). To the best of our knowledge, no previously reported cases have included PET.

Case Report

This 36-year-old woman presented with absence of sensory and motor function of both legs for 2 weeks. Her history was significant for uncontrolled tophaceous gout, for which she was taking 0.6 mg colchicine each day.

On presentation she was found to have a T7 sensory anesthesia level and lower extremity motor paralysis. Her serum uric acid level was 9.6 mg/dL.

Radiographs of the thoracic spine demonstrated absent pedicles at the T5, T6, and T7 levels (Fig 1). CT imaging revealed lytic expansile lesions of the posterior elements with associated soft tissue mass lesions involving T2–T9. Vertebral bodies were preserved.

Steroid therapy (dexamethasone 4 mg every 6 hours) was initiated with clinical improvement. MR imaging of the thoracic spine demonstrated enhancement of the mass lesion within the spinal canal and within the posterior elements (Figs 2 and 3). PET images were acquired with 17 mCi F-18 fluorodeoxyglucose (FDG). PET/MR fusion showed hypermetabolic activity involving the T5–T7 posterior elements and adjacent soft tissues (Fig 4). A CT-guided percutaneous biopsy of the posterior elements of T6 was performed (Fig 5) with sampling of the hypermetabolic tissue, which yielded soft cores of white and reddish-brown tissue that was interpreted by pathology as gouty tophi (Fig 6).

The patient underwent a surgical decompression laminectomy of levels T5–T7. She regained lower extremity sensory function with strength in the lower extremities in the immediate postoperative period. At the 10-month follow-up visit, the patient could ambulate but was hindered by pain due to her gouty arthritis elsewhere. She is no longer receiving steroid therapy, and is presently being managed on allopurinol 150 mg daily and colchicine 0.6 mg daily.



Fig 1. AP thoracic spine radiograph, demonstrating loss of left pedicles at multiple levels (arrows).

Discussion

Gout is a common metabolic disorder but is uncommonly diagnosed in the axial skeleton, with fewer than 25 cases reported in the literature. Gouty tophi have been noted to be associated with osseous erosion and destruction, intra- and extra-articular crystalline deposition, and have been known to involve the posterior elements of the spine, paraspinal soft tissues, sacroiliac joints, and even the intervertebral disk.¹ Findings in this patient included multilevel osseous destruction of the posterior spinal elements and soft tissue masses demonstrating hypermetabolism, and the major diagnostic considerations entertained before biopsy included infection, lymphoma, metastatic disease, and multiple myeloma.

Specific MR imaging findings in a group of 13 patients showed all lesions to have T1 isointensity or hypointensity, and variable signal intensity on T2 was thought to be related to the amount of calcium within the tophi.² The lesions in our patient were hypointense on both T1 and T2, which supports these findings.

Received May 19, 2005; accepted after revision July 19.

From the Departments of Radiology (T.P., J.S.C., A.T.R., G.D.M.), Neurosurgery (L.V.C.) and Pathology (H.J.W.), West Virginia University School of Medicine, Morgantown, WV.

Address correspondence to Jeffrey S. Carpenter, MD, Department of Radiology, West Virginia University School of Medicine, One Medical Center Dr, Morgantown, WV 26506.

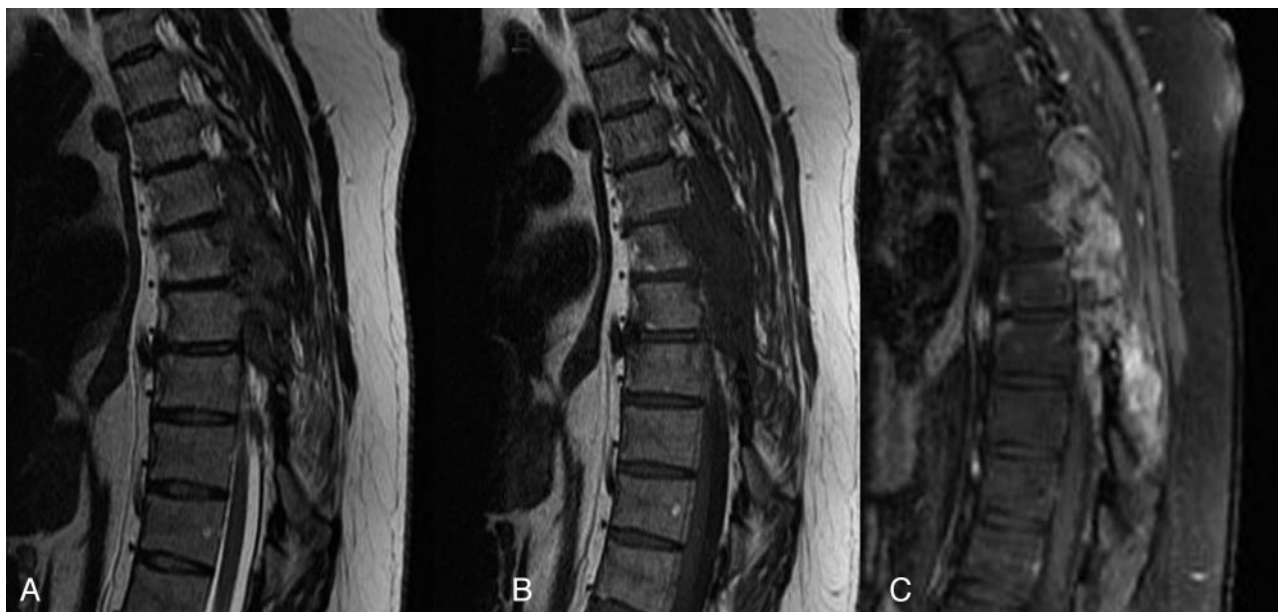


Fig 2. A, T2-weighted sagittal image (TR/TE, 4550/110) shows predominantly hypointense mass lesions replacing the posterior elements of T4 through T7. B, T1-weighted sagittal image (516/12) demonstrates hypointensity of the same lesions. C, T1-weighted fat saturation images with gadolinium (816/12) with avid enhancement of the lesions.

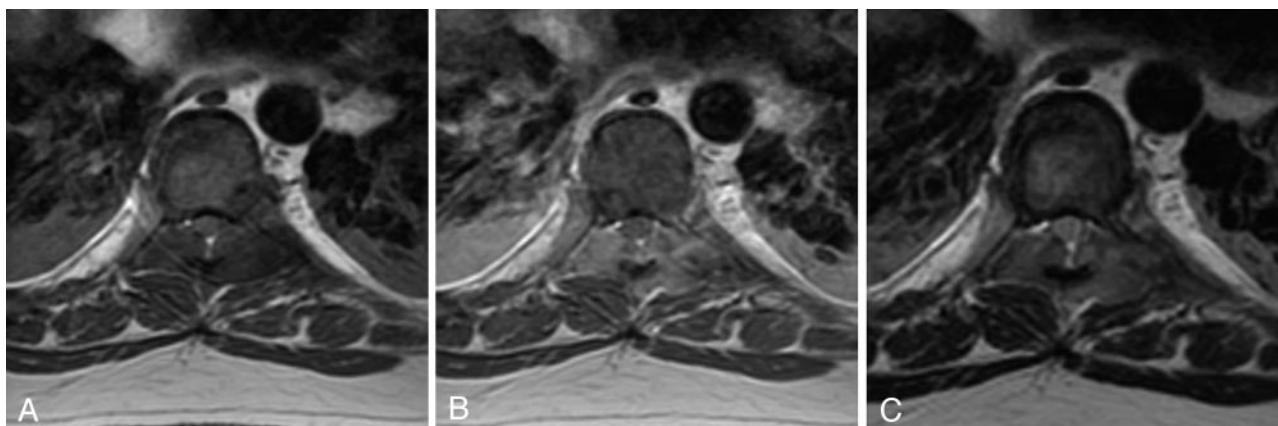


Fig 3. A, T1-weighted axial image (TR/TE, 617/10); B, T1-weighted axial image with 20 mL gadolinium (550/12) and C, T2-weighted axial image (6350/80) demonstrate extradural lesions with mass effect on the thecal sac resulting in spinal stenosis.

On CT imaging, gouty tophi have been noted to measure around 160 HU because of the monosodium urate crystal deposition.³ The attenuation of the lesions in our patient was in the range of 130–170 HU, which is consistent with previously reported findings.

FDG-PET fusion images with both MR and CT were acquired because of the differential diagnostic considerations, including metastatic disease. To the best of our knowledge, no published reports have discussed the metabolic characteristics of gout on PET. FDG-PET imaging demonstrates hypermetabolism within the lytic bone lesions and paraspinal masses.

The pathophysiology of prolonged hyperuricemia results in crystals precipitating in joint cavities. The crystals provoke an acute inflammatory response (acute gouty arthritis), which in severe cases progresses to form chalky white tophi (chronic tophaceous gout). By routine light microscopy the tophi appear as extracellular gray material surrounded by fibrous tissue and histiocytes/multinucleated giant cells. Polarized light

can be confirmatory by demonstrating the needle-shaped crystals with strong negative birefringence characteristic of gout.

Macrophages and growth factors have been shown to play a protective role in the pathophysiology of gout and in the resolution of acute gout with removal of urate crystals.^{4,5} High uptake of FDG has been related to macrophage activity and the presence of growth factors, which accounts for the intense radiotracer accumulation on FDG-PET.^{6–8} PET imaging also demonstrates excellent correlation between the regions of hypermetabolism and gadolinium enhancement.

The location of the hypermetabolic activity, within the posterior elements, with relative sparing of the vertebral bodies, should have broadened the differential diagnostic considerations initially entertained to include hypermetabolic spinal lesions such as gout, in addition to infection and neoplastic etiologies. Retrospectively, the patient's history was crucial to the diagnosis, as many of the other articles published on spinal gouty tophi state.^{2,9–18}

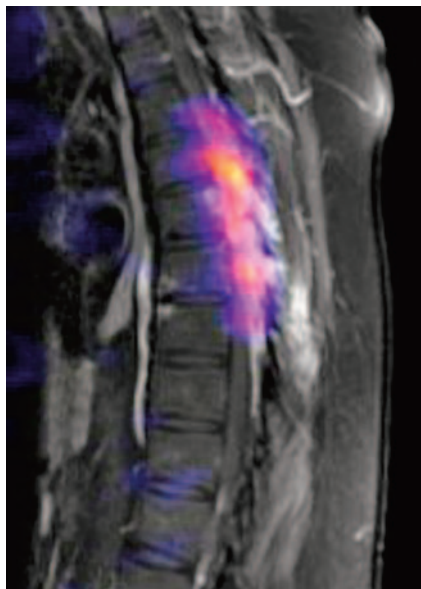


Fig 4. T1-weighted fat-saturated postcontrast images with positron-emission tomographic fusion (TR/TE, 816/12 with 20 mL gadolinium, 17 mCi F-18 FDG) demonstrate extensive hypermetabolic activity localized to the posterior elements and paraspinal soft tissues, corresponding with CT and MR mass lesions.

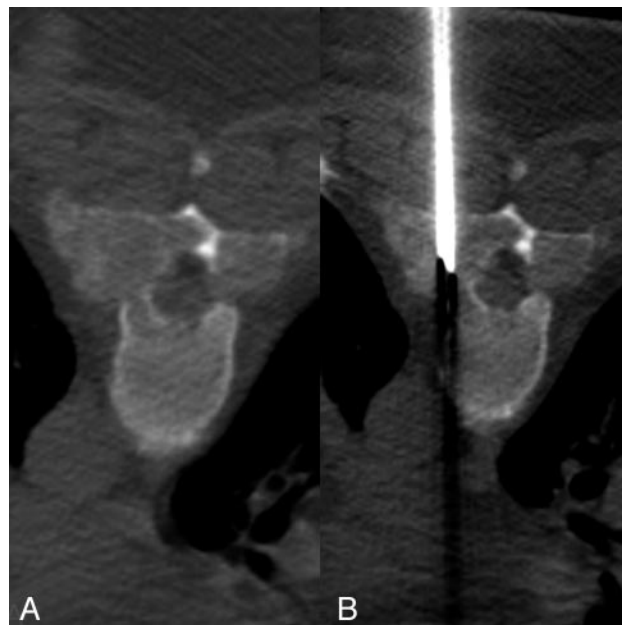


Fig 5. CT-guided percutaneous biopsy (124/552; 5.0-mm collimation, 512 × 512, 140 KV). *A*, Expansile lytic bone lesion with a soft tissue mass replacing the pedicles, lamina, and transverse processes of T6. *B*, Placement of the biopsy needle (Cook M-1 13 gauge; Cook, Bloomington, Ind) into the mass.

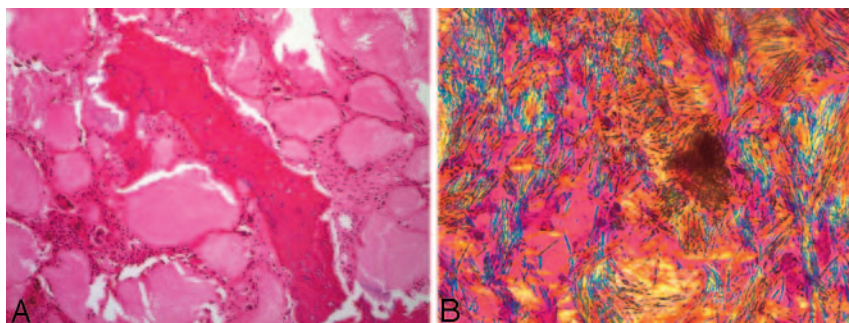


Fig 6. Pathology (*A*) central fragment of eroded bone surrounded by gouty tophi which are rimmed by multinucleated giant cells and fibrous tissue (hematoxylin-eosin ×10). *B*, Needle-shaped crystals exhibiting strong negative birefringence (bright yellow when aligned parallel with the compensating filter) characteristic of monosodium urate crystals (gout; polarized light, ×50).

References

1. Das De S. Intervertebral disc involvement in gout: brief report. *J Bone Joint Surg Br* 1988;70:671
2. Yu JS, Chung C, Recht M, et al. MR imaging of tophaceous gout. *AJR Am J Roentgenol* 1997;168:523–27
3. Gerster JC, Landry M, Dufresne L, et al. Imaging of tophaceous gout: computed tomography provides specific images compared with magnetic resonance imaging and ultrasonography. *Ann Rheum Dis* 2002;61:52–54
4. Landis RC, Yagnik DR, Florey O, et al. Safe disposal of inflammatory monosodium urate monohydrate crystals by differentiated macrophages. *Arthritis Rheum* 2002;46:3026–33
5. Yagnik DR, Evans BJ, Florey O, et al. Macrophage release of transforming growth factor beta1 during resolution of monosodium urate monohydrate crystal-induced inflammation. *Arthritis Rheum* 2004;50:2273–80
6. Ohtsuka T, Nomori H, Watanabe K, et al. False-positive findings on [18F]FDG-PET caused by non-neoplastic cellular elements after neoadjuvant chemoradiotherapy for non-small cell lung cancer. *Jpn J Clin Oncol* 2005;35:271–73
7. Defawe OD, Hustinx R, Defraigne JO, et al. Distribution of F-18 fluorodeoxyglucose (F-18 FDG) in abdominal aortic aneurysm: high accumulation in macrophages seen on PET imaging and immunohistology. *Clin Nucl Med* 2005;30:340–41
8. Ogawa M, Ishino S, Mukai T, et al. (18)F-FDG accumulation in atherosclerotic plaques: immunohistochemical and PET imaging study. *J Nucl Med* 2004;45:1106–107
9. Pfister AK, Schlarb CA, O'Neal JF. Vertebral erosion, paraplegia, and spinal gout. *AJR Am J Roentgenol* 1998;171:1430–31
10. St George E, Hillier CE, Hatfield R. Spinal cord compression: an unusual neurological complication of gout. *Rheumatology* 2001;40:711–12
11. Souza AW, Fontenele S, Carrete H Jr, et al. Involvement of the thoracic spine in tophaceous gout: a case report. *Clin Exp Rheumatol* 2002;20:228–30
12. Kao MC, Huang SC, Chiu CT, et al. Thoracic cord compression due to gout: a case report and literature review. *J Formos Med Assoc* 2000;99:572–75
13. Bret P, Ricci AC, Saint-Pierre G, et al. Thoracic spinal cord compression by a gouty tophus: case report and review of the literature. *Neurochirurgie* 1999;45:402–06
14. Duprez TP, Malghem J, Vande Berg BC, et al. Gout in the cervical spine: MR pattern mimicking diskovertebral infection. *AJNR Am J Neuroradiol* 1996;17:151–53
15. Hsu CY, Shih TT, Huang KM, et al. Tophaceous gout of the spine: MR imaging features. *Clin Radiol* 2002;57:919–25
16. Sato J, Watanabe H, Shinozaki T, et al. Gouty tophus of the patella evaluated by PET imaging. *Acta Neurochirurgica* 1998;140:729–30
17. Mahmud T, Basu D, Dyson PH. Crystal arthropathy of the lumbar spine: a series of six cases and a review of the literature. *J Bone Joint Surg Br* 2000;87:513–17
18. Kelly J, Lim C, Kamel M, et al. Topacheous gout as a rare cause of spinal stenosis in the lumbar region: case report. *J Neurosurg Spine* 2005;2:215–17